THE JOURNAL OF BIOLOGICAL CHEMISTRY VOL. 291, NO. 21, pp. 11434–11445, May 20, 2016

Site-specific Acetylation of Histone H3 Decreases Polymerase β Activity on Nucleosome Core Particles *in Vitro*[*][S]

Received for publication, March 7, 2016, and in revised form, March 28, 2016 Published, JBC Papers in Press, March 31, 2016, DOI 10.1074/jbc.M116.725788

Yesenia Rodriguez[1], **John M. Hinz, Marian F. Laughery, John J. Wyrick, and Michael J. Smerdon**[2]

From Biochemistry and Biophysics, School of Molecular Biosciences, Washington State University, Pullman, Washington 99164-7520

Histone posttranslational modifications have been associated with changes in chromatin structure necessary for transcription, replication, and DNA repair. Acetylation is one of the most studied and best characterized histone posttranslational modifications, but it is not known if histone acetylation modulates base excision repair of DNA lesions in chromatin. To address this question, we generated nucleosome core particles (NCPs) containing site-specifically acetylated H3K14 or H3K56 and measured repair of uracil and single-nucleotide gaps. We find that H3K56Ac and H3K14Ac do not significantly contribute to removal of uracils by uracil DNA glycosylase regardless of the translational or rotational position of the lesions within NCPs. In repair of single-nucleotide gaps, however, the presence of H3K56Ac or H3K14Ac in NCPs decreases the gap-filling activity of DNA polymerase β near the dyad center, with H3K14Ac exhibiting stronger inhibition. To a lesser extent, H3K56Ac induces a similar effect near the DNA ends. Moreover, using restriction enzyme accessibility, we detect no changes in NCP structure or dynamics between H3K14Ac-NCPs and WT-NCPs containing single-nucleotide gaps. Thus, acetylation at H3K56 and H3K14 in nucleosomes may promote alternative gap-filling pathways by inhibiting DNA polymerase β activity.

Eukaryotic DNA is organized into arrays of nucleosomes, which constitute the primary level of chromatin compaction. Vital DNA-templated processes, including transcription and DNA repair, are dependent on protein-DNA interactions, which are restricted by the histone proteins in nucleosomes. The nucleosome core particle (NCP)[3] consists of 147 bp of DNA wrapped ~1.7 times around a histone octamer composed of a tetramer of histones H3 and H4 ($(H3\text{-}H4)_2$) flanked by two heterodimers of histones H2A and H2B (H2A-H2B) (1). Accessibility of nuclear factors to occluded DNA in this stable, yet dynamic protein-DNA complex is regulated by multiple mechanisms, including the activity of chromatin remodeling complexes (2, 3) and the intrinsic, partial unwrapping of DNA ends from the histone octamer (4, 5).

The rate of DNA unwrapping, also referred to as DNA breathing, in nucleosomes is dependent on DNA sequence and the posttranslational modification (PTM) status of the histones (6–8). Acetylation of lysine 56 on histone H3 (H3K56) has been shown to increase unwrapping dynamics (9, 10). Conflicting results have been reported on the extent of this unwrapping or how far into the nucleosome core the DNA transiently dissociates (9, 10). Presumably, these differences are due to the different assays used, where DNA dissociation as far as 27 bp from the DNA ends may occur via cooperativity of adjacent target sites (10). It is nonetheless evident that DNA dissociation occurs at least within the last turn of the DNA ends on the nucleosome core in the absence of DNA-binding proteins whose target sites extend beyond this region (9). The lysine residue at this site electrostatically interacts with the phosphate backbone of the DNA and, when acetylated (H3K56Ac), imparts nucleosome disruption directly via charge neutralization. *In vivo*, tight regulation of H3K56Ac is critical for genome stability. Newly synthesized histone H3 molecules incorporated into chromosomes are acetylated at Lys-56 by the histone acetyltransferase Rtt109 (in yeast) or p300/CBP (in humans) during S phase (11, 12). In the absence of DNA damage, the NAD^+-dependent histone deacetylases Hst3 and Hst4 largely remove this modification in G_2 (13–16). Defects in the regulation of H3K56Ac render eukaryotic cells sensitive to genotoxic agents that interfere with DNA replication (thereby inducing DNA strand breaks), including methyl methanesulfonate (MMS) and camptothecin (12, 17, 18).

Importantly, the structural location of histone acetylation has been shown to be a strong determinant of the mechanism by which nucleosome disruption occurs. In general, acetylation of lysine residues within the globular domain of histone H3 impact nucleosome structural stability. For example, acetylation near the DNA entry/exit points on NCPs regulates the DNA unwrapping dynamics, and lysine acetylation near the central dyad promotes NCP disassembly (19). On the other

* This work was supported by National Institutes of Health Grants ES020955 (to J M. H.), ES002614 and ES004106 (NIEHS; to M. J. S.), and Training Grant T32GM008336 (NIGMS; to Y. R.). The authors declare that they have no conflicts of interest with the contents of this article. The content is solely the responsibility of the authors and does not necessarily represent the official views of the National Institutes of Health.

[S] This article contains supplemental Tables S1 and S2 and Figs. S1–S6.

[1] Present address: Genome Integrity and Structural Biology Laboratory, NIEHS, National Institutes of Health, P. O. Box 12233, Mail Drop F3-01, Research Triangle Park, NC 27709.

[2] To whom correspondence should be addressed: School of Molecular Biosciences, Life Sciences and Biotechnology Building, Washington State University, Pullman, WA. Tel.: 509-335-6853; Fax: 509-335-4159; E-mail: smerdon@wsu.edu.

[3] The abbreviations used are: NCP, nucleosome core particle; PTM, posttranslational modification; H3K56, lysine 56 on histone H3; H3K56Ac, acetylated lysine 56 on histone H3; MMS, methyl methanesulfonate; H3K14, lysine 14 on histone H3; H3K14Ac, acetylated lysine 14 on histone H3; DSB, double strand break; BER, base excision repair; UDG, uracil DNA glycosylase; Pol β, polymerase β; PARP1, poly(ADP-ribose) polymerase-1; PCI, phenol:chloroform:isoamyl alcohol; *Mb*, *Methanosarcina barkeri*; NTA, nitrilotriacetic acid; CI, chloroform:isoamyl alcohol; RE, restriction enzyme; AP, abasic.

hand, histone acetylation in the very basic N-terminal tails primarily influences chromatin structure indirectly by the recruitment of bromodomain-containing factors that recognize acetylated lysines. For example, the Rsc4 subunit of the ATP-dependent chromatin remodeler RSC (remodels the structure of chromatin) contains tandem bromodomains that specifically bind the acetylated lysine 14 of histone H3 (H3K14), located in the N-terminal tail of H3 (20, 21). It was also reported that acetylation at H3K14 is important for DNA damage checkpoint activation by directly regulating chromatin structure through the activity of RSC in fission yeast (22). Indeed, hyperacetylation at H3K14 and/or H3K9 is induced after ultraviolet (UV) irradiation in yeast (23). Furthermore, H3K14Ac is an essential mark for histone octamer eviction from promoter DNA by the histone chaperone Nap1, which is necessary for transcriptional activation (24); however, the molecular mechanism of how H3K14Ac regulates nucleosome dynamics during DNA repair is not known.

There is a growing body of work supporting the role of histone PTMs in altering chromatin structure and promoting efficient DNA repair (25), with the majority of DNA damage-inducible histone PTMs known to date being studied in the context of double-strand break (DSB) repair and nucleotide excision repair. However, little is known about how these modifications influence the essential DNA repair process of base excision repair (BER). BER is responsible for repairing the most abundant types of endogenous damage, including chemically modified bases, errant uracil residues, abasic (AP) sites, and single-strand breaks (26). BER occurs in a coordinated, stepwise process, initiated by the recognition of chemically modified bases by one of a number of glycosylases that cleave the *N*-glycosidic bond, removing the damaged base from DNA and leaving an AP site intermediate (27). The AP site is recognized by the primary abasic site endonuclease, APE1, which cleaves the DNA backbone on the 5′ side of the AP site (26, 27). The repair polymerase Pol β removes the abasic deoxyribose phosphate from the single-strand break intermediate and replaces the missing nucleotide using the intact strand as a template (26, 28). Finally, the nicked DNA strand is ligated by ligase I or the ligase IIIα-XRCC1 complex, completing the repair process and restoring DNA integrity (29, 30).

Many studies have now found that, in the context of nucleosomes, the structural location of the DNA lesion greatly impacts the activity of all BER enzymes *in vitro*, including different DNA glycosylases, APE1, and Pol β (31–38). Thus, site-specific acetylation of histones may influence BER in a manner that is linked to the structural location of the DNA lesion. Furthermore, in the cell it is unlikely that the process of BER occurs in the absence of histone modifications. Unlike the repair of DNA DSBs, there is as of yet no direct evidence of histone modifications associated with the repair of DNA lesions recognized by the glycosylases of BER. However, proteins that regulate histone acetylation status, such as SIRT6 (an NAD^+-dependent histone/protein deacetylase) and ADP-ribosyltransferase from the sirtiun family, have been found to be involved in regulating BER *in vivo*. SIRT6 specifically targets H3K9 and H3K56 deacetylation, which promotes poly(ADP-ribose) polymerase-1 (PARP1) activation and repair (39). $SIRT6^{-/-}$ mouse embryonic fibroblasts exhibit hyperacetylation at these sites and are sensitive to MMS and H_2O_2 (40). Sensitivity to these agents can be rescued by overexpression of the 8-kDa, lyase domain of Pol β (40). Furthermore, it was recently reported that SIRT6 interacts with MYH, a DNA glycosylase, and APE1 and stimulates their activity (41). These results suggest that the potential regulation of BER via histone modification may require "'fine-tuning" of histone acetylation/deacetylation levels to regulate BER activities. Therefore, in addition to regulation of chromatin dynamics, histone acetylation may be important for recruitment of factors that directly regulate the activity of BER factors.

Because nucleosome structure has a strong impact on BER in the removal of uracil, it is feasible that factors that could change chromatin structure, such as site-specific acetylation, may influence the accessibility of BER enzymes to their target sites. In this study we use NCPs consisting of one of two homogeneously acetylated H3 histones (H3K56 and H3K14) to measure their effect on the activities of uracil DNA glycosylase (UDG) and Pol β at structurally positioned uracils and single-nucleotide gaps, respectively. Furthermore, two different nucleosome positioning DNA sequences were used to explore a wider range of histone octamer binding affinities that may exist in eukaryotic cells. The 601 DNA positioning sequence has a strong binding affinity and generates homogeneously positioned NCPs, allowing us to discern the effects due to translational positioning of the lesion relative to the site of modification (42). The *Xenopus borealis* 5S rDNA sequence, on the other hand, positions the histone octamer along the DNA at two major positions due to its reduced binding affinity for the histone octamer and yields a more "translationally flexible" NCP than the 601 sequence.

Our results indicate that acetylation at either H3K56 or H3K14 has little effect on the removal of uracil by UDG/APE1 regardless of the rotational or translational position in NCPs. However, H3K14Ac and H3K56Ac unexpectedly decrease the gap-filling activity of Pol β by 2–5-fold when the DNA gap is positioned near the central dyad axis and to a lesser extent when the DNA gap is positioned near the DNA ends. Thus, although histone acetylation is associated with an "open" chromatin structure *in vivo* and increased nucleosome dynamics *in vitro*, this study emphasizes that the role of histone site-specific acetylation is context-dependent and may be important for recruitment of BER-associated proteins, such as ATP-dependent chromatin remodeling factors.

Experimental Procedures

Preparation of DNA Substrates Containing Uracil and Single-nucleotide Gaps—The 147-bp 601 nucleosome positioning DNA sequence (43) was slightly modified to introduce a single uracil at distinct positions as reported previously (31). Five synthetic oligomers were purchased from Integrated DNA Technologies (IDT), four of which contained a single uracil in the strand corresponding to the I chain in the NCP 601 crystal structure reported by Vasudevan *et al.* (44). Nomenclature of the substrates follows the same convention as reported previously (31), and the substrates are listed in supplemental Table S1 for the 601-NCPs and in supplemental Table S2 for the

5S-NCPs. Each of the uracil-containing oligonucleotides was radiolabeled with [γ-^{32}P]ATP (PerkinElmer Life Sciences) at the 5′ end using T4 polynucleotide kinase (Invitrogen) and annealed (1:1) with the complementary partner strand by heating to 95 °C for 10 min and slow cooling in a buffer containing 30 mM Tris, pH 7.5, and 100 mM potassium acetate. The generated dsDNA was then purified using the QIAquick Nucleotide Removal kit or the PCR purification kit (Qiagen) to remove excess unincorporated radioactive nucleotides. For the substrates containing the 5S nucleosomal positioning sequence, a 196-bp DNA substrate was generated by PCR using the plasmid pKS-5S as a template as described in Mann *et al.* (45). The forward primers contained a single uracil, whereas the reverse primer contained a biotin tag at its 5′ end to allow for selective radioactive labeling of the uracil-containing strand after PCR. The PCR product was purified from agarose gels after electrophoresis using a gel extraction kit (Qiagen). The single-nucleotide gap DNAs were generated from the uracil-containing DNAs by treatment with UDG and APE1 (New England BioLabs; 30 nM and 10 nM, respectively) for 90 min at 37 °C to ensure the cleavage of all uracil residues and subsequent cleavage of the abasic sites. The DNA was then treated 1:2 (v/v) with phenol:chloroform:isoamyl alcohol (PCI; 25:24:1) followed by a chloroform:isoamyl alcohol extraction (24:1) and standard ethanol precipitation.

Nucleosome Core Particle Reconstitutions—NCPs were reconstituted by salt gradient dialysis using recombinant octamer from *Xenopus laevis* containing unmodified wild type (WT) core histones or histone H3 acetylated at Lys-14 or Lys-56. First, for the isolation of the WT core histones, each histone was individually expressed in *Escherichia coli* (BL21) as previously described (46) with some modifications described in Duan and Smerdon (47). After isolation, the histones were subjected to dialysis with deionized water containing 5 mM 2-mercaptoethanol and 0.2 mM PMSF. They were then lyophilized until dry, and the histone octamer was prepared as described by Luger *et al.* (46). Briefly, the concentration of the unfolded histone proteins was determined at A_{276}, and equimolar ratios of all four histones were mixed and dialyzed three times in refolding buffer (2 M NaCl, 20 mM Tris-HCl, pH 7.5, 1 mM Na-EDTA, 5 mM 2-mercaptoethanol) at 4 °C. Generation of homogeneous histone octamers containing either H3K14Ac or H3K56Ac was performed as described previously in Neumann *et al.* (9). Briefly, BL21 *E. coli* were cotransformed with a plasmid (pAcKRS-3) containing the ORF of the gene directing the synthesis of acetyllysine-tRNA synthetase from *Methanosarcina barkeri (Mb)*, which directs insertion of acetyllysine residues at amber codons, and plasmid (pCDF PyIT-1) containing the *Mb*tRNA$_{CUA}$ gene and an N-terminally hexahistadine-tagged histone H3, encoding an amber codon at position 14 or 56, downstream of a T7 promoter (both plasmids were generous gifts from Dr. Jason Chin, Medical Research Council Laboratory of Molecular Biology). BL21 *E. coli* transformed with these two plasmids were grown overnight, and when A_{600} reached ~0.8, they were supplemented with 10 mM acetyllysine and 20 mM nicotinamide (to inhibit the *E. coli* deacetylase CobB). Thirty minutes later protein expression was induced by IPTG addition. Cells were allowed to grow an additional 3–3.5 h, and histone purification was performed via nickel-NTA chromatography. This was followed by the removal of the N-terminal His$_6$ tag with tobacco etch virus protease as described (9). Radiolabeled DNA was then mixed with site-specific acetylated or WT histone octamer in a 1:1.2 molar ratio via salt gradient dialysis to reconstitute NCPs as described (31, 47).

Hydroxyl-radical Footprinting—Hydroxyl-radical footprinting of NCPs was performed as previously described (36, 48). The hydroxyl radical reaction with NCPs was performed at room temperature and quenched after 10 min with glycerol to a final concentration of 6%. The DNA was isolated from the histones via PCI, 25:24:1 (v/v), extraction followed by a chloroform:isoamyl alcohol, 24:1 (v/v) (CI), wash. The DNA was then ethanol-precipitated overnight. The DNA pellet was washed twice with 70% ethanol, air-dried, and resuspended in 1× Tris EDTA and Hi-Di^{TM} formamide (Applied Biosystems). Uracil-containing DNA was treated with UDG (30 nM) and APE1 (10 nM), and incubated at 37 °C for 90 min for total cleavage to take place. Cleavage reactions were also ethanol precipitated overnight. Samples were boiled for 10 min to denature the DNA, chilled on ice, and separated by electrophoresis in an 8% denaturing (7 M urea) polyacrylamide (19:1) gel. The gel was run at 60 W for 2.5 h, dried, exposed on a phosphor screen, and visualized on Typhon FLA 7000 phosphorimaging (GE Healthcare). Analysis of the image was performed using ImageQuant TL (GE Healthcare).

UDG and APE1 Cleavage Measurements—WT and acetylated NCPs (20 nM) were treated with *E. coli* UDG and human APE1 (New England Biolabs) at concentrations shown in the figures. These cleavage reactions were performed in the presence of repair reaction buffer containing 25 mM HEPES (pH 7.5), 2 mM DTT, 100 μg/ml BSA, 10% glycerol, 5 mM $MgCl_2$, 200 μM EDTA (pH 8), and 4 mM ATP. Reaction mixtures were incubated at 37 °C for the specified times from 0 to 60 min, and reactions were terminated by adding PCI (1:2, sample: PCI, v/v). DNA was ethanol-precipitated, resuspended in 1× Tris-EDTA, and mixed with an equal volume of formamide-containing loading buffer. Digested products were separated by electrophoresis on 10% polyacrylamide (19:1), 7 M urea denaturing gels in 1× Tris borate-EDTA buffer. Gels were exposed on a phosphor screen and visualized on Typhoon FLA7000 (GE Healthcare). Analysis of the image was performed using ImageQuant (IQ) TL software.

Pol β Gap-filling Assays—Extension activity by Pol β was assessed using two methods (the one-label and two-label assays) that have been described previously (31). Briefly, in the two-label assay, the complementary strand (partner strand) of the gapped DNA was radiolabeled at its 5′ end and annealed (1:1) with its complementary uracil-containing strand. The DNA was then treated with UDG (30 nM) and APE1 (10 nM) for 90 min at 37 °C to ensure cleavage of all uracils. The cleaved substrate was then reconstituted into NCPs as described above. After the reconstitution efficiency was confirmed, the Pol β repair reaction was immediately performed. The repair reaction mixture contained gapped NCP (20 ng), repair reaction buffer (31), [α-^{32}P]dCTP at 40 nCi/μl (PerkinElmer Life Sciences), and freshly diluted Pol β to a final concentration of 5 nM. Reaction mixtures were incubated at 37 °C for the specified

times and quenched using PCI. Extension products were separated on 10% polyacrylamide (19:1) 7 M urea denaturing gels in 1× Tris borate-EDTA buffer. Visualization and analysis were performed using Typhoon FLA7000 and IQTL, respectively. In the second method used, one-label assay, the uracil-containing strand was radiolabeled at its 5′ end, and the gapped NCP substrate was generated as described above. The repair reaction was then performed as previously described except that nonradioactive dCTP (100 μM) was used. All extension products were separated in a denaturing sequencing gel containing 8% polyacrylamide (19:1) and 7 M urea in 1× Tris borate-EDTA buffer, and the percent extended was calculated as described (31). Normalized data from either assay were fitted to a single-phase exponential curve using GraphPad Prism v.6 and the equation $Y = Y_{max}\ (1 - e^{-k_{obs}t})$ as previously performed by others (33, 49). The initial rates are reported in Table 1.

Restriction Enzyme Accessibility Assay—Restriction enzymes HaeIII and HhaI (New England Biolabs) cleaving at restriction sites corresponding to +51 and +2, respectively, were used to determine the accessibility of these sites in intact and gap-containing NCPs (WT and H3K14Ac) at two sites: gI (+4) and gO (+10) where "I" and "O" correspond to the "in" and "out" rotational orientation of the DNA gap (g) relative to the histone octamer surface, respectively. Gapped DNAs and NCPs were incubated with 10 units of each enzyme at 37 °C for 2 h followed by standard PCI and CI isolation of DNA. Cleavage products were separated on a 16% non-denaturing gel, and visualization and quantification of results were performed as described above.

Yeast MMS Sensitivity Assays—Mutations in histone H3 K14R and K56R were constructed in plasmid pJW500 (50) by site-directed mutagenesis following our published protocol (50). Histone mutations were confirmed by sequencing and then introduced into yeast strain WY500 (50) by plasmid shuffling. To assess the sensitivity of histone H3 K14R, H3 K56R, and H3 K14R/K56R mutants to MMS, strains were cultured overnight in yeast extract/peptone/dextrose media. Serial dilutions of the cultures were then made in yeast extract/peptone/dextrose media and spotted onto freshly poured Synthetic Complete (SC) plates containing MMS (Aldrich). Plates were incubated 3 or 4 days at 30 °C before taking pictures.

Results

Assembly of Nucleosome Core Particles Is Independent of H3K14 and H3K56 Acetylation—We and others have previously reported that the presence of a single uracil does not affect the efficiency of NCP reconstitution using histone octamers isolated from chicken erythrocytes (31–33). In this study we reconstituted NCP substrates with DNAs containing a single uracil or nucleotide gap with inward and outward rotational orientations using either unmodified recombinant histone octamers (WT) or histone octamers containing homogeneously acetylated H3 (H3K14 or H3K56). We find that these different reconstituted NCPs yield the same electrophoretic mobility shift on native gels regardless of DNA lesion position and/or location of either histone site-specific acetylation (supplemental Fig. S1), indicating nucleosome formation is not affected by acetylation of either lysine. These results are in agreement with previous findings that indicate reconstitution efficiency is not affected in hyperacetylated octamers from HeLa cells (51). The rotational setting of these DNA lesions was previously verified by hydroxyl radical footprinting of unacetylated (or WT) NCPs (31). Notably, we find that H3K14Ac does not change the rotational orientation of DNA on the histone octamer surface in the presence of a single nucleotide gap (601-NCP-gI (+4)) (supplemental Fig. S2).

Effects of Rotational and Translational Positioning on Uracil Removal by UDG and APE1 Are Independent of H3K14 and H3K56 Acetylation—We characterized how the two distinct histone H3 acetylations (H3 K14Ac and H3 K56Ac) affected BER of nucleosomal substrates. These acetylation sites were chosen for study because they target distinct regions of the nucleosome (*i.e.* histone core *versus* flexible histone tail) and have different effects on MMS sensitivity in budding yeast. Mutation of H3 Lys-56 to arginine in *Saccharomyces cerevisiae* renders cells hypersensitive to MMS (supplemental Fig. S3), in agreement with previous reports (52, 53), indicating that H3 Lys-56 acetylation may be associated with BER of MMS-induced DNA lesions. In contrast, an H3 K14R mutant in budding yeast does not affect MMS sensitivity in either a WT or H3 K56R mutant background (supplemental Fig. S3). Interestingly, this mutation in fission yeast was shown to be sensitive to MMS (22). However, H3 Lys-14 acetylation is linked to other repair pathways, including nucleotide excision repair of UV-induced DNA lesions (23). Therefore, we wanted to determine if site-specific acetylation at H3K14 and H3K56 differentially influences the activity of BER enzymes.

The structural locations of the histone acetylation and DNA lesion sites that were examined are shown in Fig. 1. As can be seen in Fig. 1*A*, Lys-14 is located in the N-terminal tail of H3, whereas Lys-56 is located in the histone fold domain near the DNA entry-exit region of NCPs. Furthermore, the DNA substrates NCP-UI (+4) and NCP-UO (+10) are in closer proximity to these acetyllysines than those lesions near the DNA ends (NCP-UI (−49) and NCP-UO (−35)). We note that the 5S-NCPs (Fig. 1, *B* and *C*) were reconstituted with a longer DNA fragment to accommodate the alternate translational positions, and both DNA lesions (labeled In (−47) and Out (−67)) are located near the DNA ends. Additionally, because the translational position of these lesions will vary by increments of ~10 bp, these alternate positions should preserve the rotational setting of lesions while being more (or less) influenced by DNA breathing. To determine the effect of these acetyllysines on the initiation of BER, NCP substrates were treated with UDG (in the presence of APE1), and cleavage of the uracil-containing strand was measured over time (we note that a non-rate-limiting concentration of APE1 was used to cleave the DNA at sites where uracil was removed by UDG).

We found that, independent of the location of uracil, acetylation at H3K14 or H3K56 does not have a significant effect on the activity of UDG (Fig. 2). Given that the effects of H3K56Ac are less likely to influence the removal of DNA lesions near the dyad (19), we only determined the effect of H3K56Ac near the DNA ends for the inwardly oriented (occluded) uracil (−49). However, the direct increase in DNA unwrapping afforded by H3K56Ac is not sufficient to increase accessibility to BER pro-

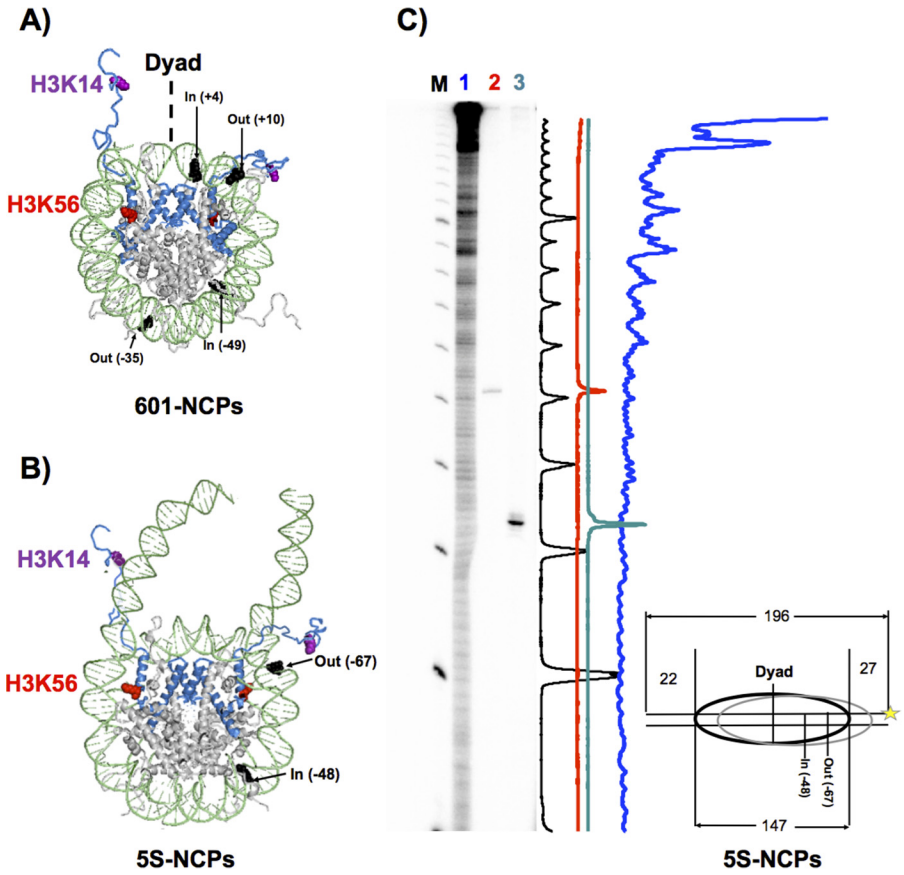

FIGURE 1. **Positioning of uracils and single-nucleotide gaps relative to histone H3 site-specific acetylation in reconstituted nucleosomes.** *A* and *B*, the NCP crystal structure (Protein Data Bank code IKX5) was modified to highlight the location of DNA lesions, uracil, and single nucleotide gaps (shown in *black*), and sites of histone acetylation. The two histone H3 proteins shown in *blue*, with residue H3K14 highlighted in *magenta* and H3K56 in *red*. The rotational orientation of lesions is denoted as *In* or *Out* when the DNA backbone faces the histone octamer or the solvent, respectively. *Numbers in parenthesis* indicate the number of nucleotides from the 5′ end (+) or 3′ end (−) of the dyad center of symmetry, which is designated as translational position 0. Position 0 for the 5S-NCPs was designated relative to the "predominant" translational position previously reported (54). For the 5S-NCPs, DNA lesions are located in the transcribed strand of a 196-bp fragment of rDNA containing the *X. borealis* somatic 5 S rRNA gene. *C*, hydroxyl radical footprint of the damaged DNA strand of 5S-NCPs, radiolabeled at the 5′ end and reconstituted with recombinant WT histones. Hydroxyl radical footprinting reactions were carried out as described under "Experimental Procedures," and the reaction products separated on DNA sequencing gels. *Lane M*, ^{32}P end-labeled 10-bp DNA ladder. *Lane 1*, 5S-NCP-UI (−48) exposed to hydroxyl radical reaction. *Lanes 2* and *3*, 5S-rDNA containing UI (−48) or UO (−67), respectively, treated with UDG and APE1, which cleaves 5′ to the AP site, generating uracil-cleavage bands 1 nucleotide longer than the same positions in the hydroxyl radical footprint scans of the gel shown on the *right*. The color of each scan is denoted by the color of the lane number. *C*, *schematic*, *bottom right* shows the translational positions of the histone octamer along the 196-bp 5S DNA substrate. The translational positions of the DNA lesions was assigned relative to the labeled transcribed strand (*yellow star*) of the predominant NCP position (*solid black oval*).

teins to that lesion despite being located just 25 bp from the DNA ends (Fig. 2*A*). We observed similar results for the 5S-NCPs (Fig. 2, *B* and *C*), where acetylation does not influence uracil removal. However, uracils in the 5S-NCPs are more amenable for repair as compared with 601-NCPs. At 150× lower UDG concentration, 5S-NCP-UI (−48) is more efficiently removed compared with 601-NCP-UI (−49) (Fig. 1, *A* and *B*). In agreement with these results, we also found that acetylation has no measurable effect on removal of the two lesions near the dyad in NCPs assembled with the positioning sequence TG-GRE-TG (36) (supplemental Fig. S4)

Taken together, our results indicate that histone acetylation at H3K14 and H3K56 does not induce significant structural and/or dynamic changes to influence the recognition and removal of uracil by UDG and APE1. We note that the effects of translational and rotational positioning on the repair efficiency of UDG/APE1 in the unmodified recombinant octamer are consistent with the effects we previously observed using chicken histones (31).

The Extension Activity of Polymerase β Is Dependent on the Structural Location of the DNA Gap and Histone Site-specific Acetylation—Given that Pol β is more strongly inhibited in NCPs than UDG (31), small changes to nucleosome structure and/or dynamics due to acetylation are more likely to impact Pol β activity. To determine a possible effect of site-specific histone acetylation on the gap-filling activity of Pol β, we first used a single-label DNA extension assay (31). In this assay NCPs are incubated with Pol β, in excess relative to the substrate (Fig. 3, *A*–*C*), to determine the single-nucleotide extension of substrate relative to total substrate in the reaction. Because Pol β is not in limited amounts, results of the assay are more reflective of the DNA synthesis step rather than substrate binding of the enzyme. Gap-containing DNAs were generated by pretreating 5′ end-labeled uracil-containing DNAs with UDG and APE1. The cleaved DNA substrates were reconstituted with recombinant octamers containing WT histones or octamers containing H3K14Ac or H3K56Ac. The NCP substrates were incubated for different times with 100 nM Pol β;

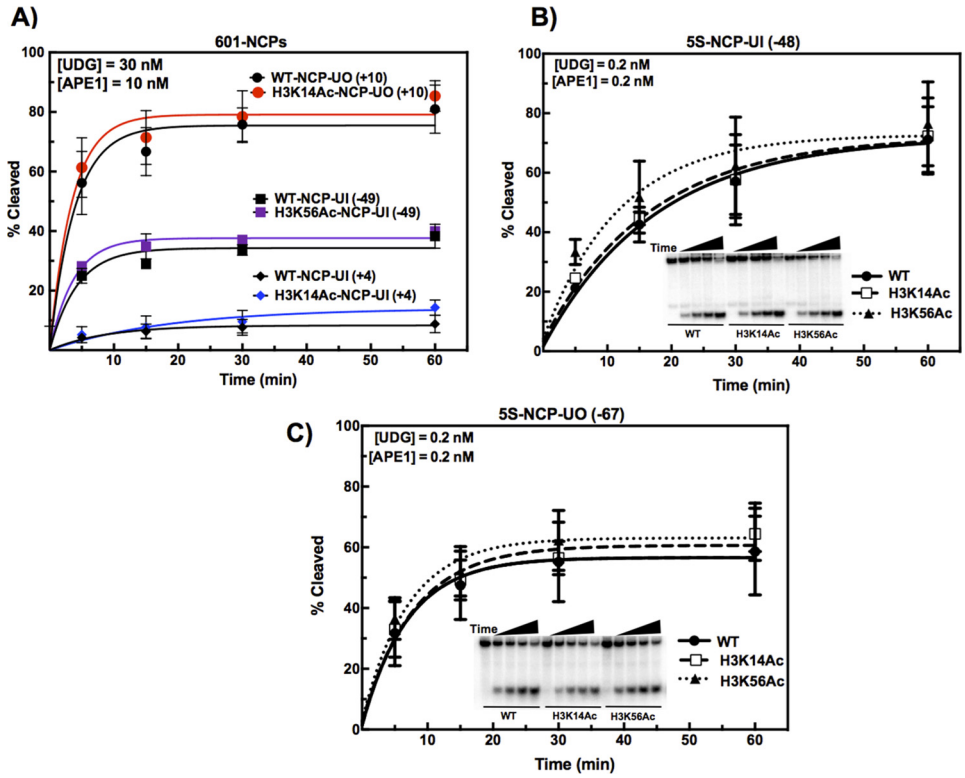

FIGURE 2. **Effect of histone site-specific acetylation on the removal of rotationally and translationally positioned uracil in nucleosomes.** NCPs containing acetylated (H3K14 or H3K56) or unmodified (WT) histone octamers and either the 601 DNA (*A*) or 5S rDNA (*B* and *C*) containing a single uracil at the specified locations (in *parentheses in the panels*) were incubated with UDG and APE1 for the specified times (enzyme concentrations are given in the plots). Data points represent the mean ± 1 S.D.) of three independent experiments and are fitted to a single-phase exponential curve as described under "Experimental Procedures." For data points where no error bars were visible, the S.D. was smaller or similar in magnitude to the size of the symbol.

reaction products were separated in a DNA sequencing gel, and the percentage of substrate extended was quantified as described under "Experimental Procedures." Surprisingly, acetylation at either H3K14 or H3K56 decreased the total amount of substrate that Pol β can extend, as seen by a decrease in Y_{max} at the outward oriented gap near the dyad (+10), with H3K14 having a stronger inhibition (Fig. 3*A*). However, Pol β activity at inwardly oriented gaps near the dyad (Fig. 3*B*) or near the DNA ends (Fig. 3*C*) was independent of acetylation status. The corresponding initial rate of product formation, given in Table 1, in the acetylated H3K14 at this site is ~3-fold lower compared with the WT. Acetylation did not have a significant effect on Pol β activity at inwardly oriented gaps near the dyad (Fig. 3*B*) or near the DNA ends (Fig. 3*C*).

Because the amount of substrate that Pol β is able to extend is quickly consumed during these experiments, accurate initial rate calculations were not possible. Nonetheless, our data illustrate that although the 601-NCPs are homogeneously positioned, there is a small population that is more amenable for repair. However, >65% of the 601-NCPs with gaps near the dyad center strongly inhibited Pol β extension (Fig. 3, *A*–*C*). Importantly, histone acetylation at either site is not sufficient to relieve this inhibition and, in fact, decreased the amount of functional substrate at an outwardly oriented gap near the dyad (Fig. 3*A*). This may reflect a direct affect on NCP stability and/or dynamics (*e.g.* by increasing local rotational dynamics and, therefore, decreasing the average time the lesion is fully outwardly oriented). Alternatively, acetylation may promote "unproductive binding" of Pol β to the substrate, resulting in a decrease of functional substrate.

To determine if histone site-specific acetylation had a similar effect under conditions where Pol β is limiting relative to the nucleosomal substrate, we used a two-label assay (Fig. 4, *A*–*C*) in which we first 5′ end-labeled the undamaged strand and then measured Pol β incorporation of [α-^{32}P]dCTP relative to the signal in the undamaged strand (31). This assay is more sensitive than the Pol β extension assay, allowing the use of smaller amounts of Pol β with excess nucleosomal substrate (*i.e.* a better representation of *in vivo* conditions) to study Pol β activity under steady-state conditions. Because the 5S-NCPs are more amenable for repair, even small amounts of product generated in steady-state conditions can be detected using the one-label assay (Fig. 4*D*). As mentioned earlier, acetylation at H3K56 is associated with increased DNA unwrapping within one turn of the DNA ends (9). Therefore, we focused on the effect of this modification on lesions further away from the dyad center. We found that H3K56Ac decreased Pol β extension activity by ~2-fold at NCP-gO (+10) (Fig. 4*A*). Similarly Pol β activity was decreased at NCP-gO (−35) (Fig. 4*B*). However, acetylation at this site had little effect on the amount of product formed at NCP-gI (−49) (Fig. 4*C*) or in the 5S-NCPs (Fig. 4*D*). Interestingly, under these Pol β-limiting conditions, H3K14 acetylation decreased the total amount of product formed (Y_{max}) by ~2-fold at NCP-gI (+4) (Fig. 5*A*) while having no effect on Pol β activity at NCP-gO (+10) (Fig. 5*B*).

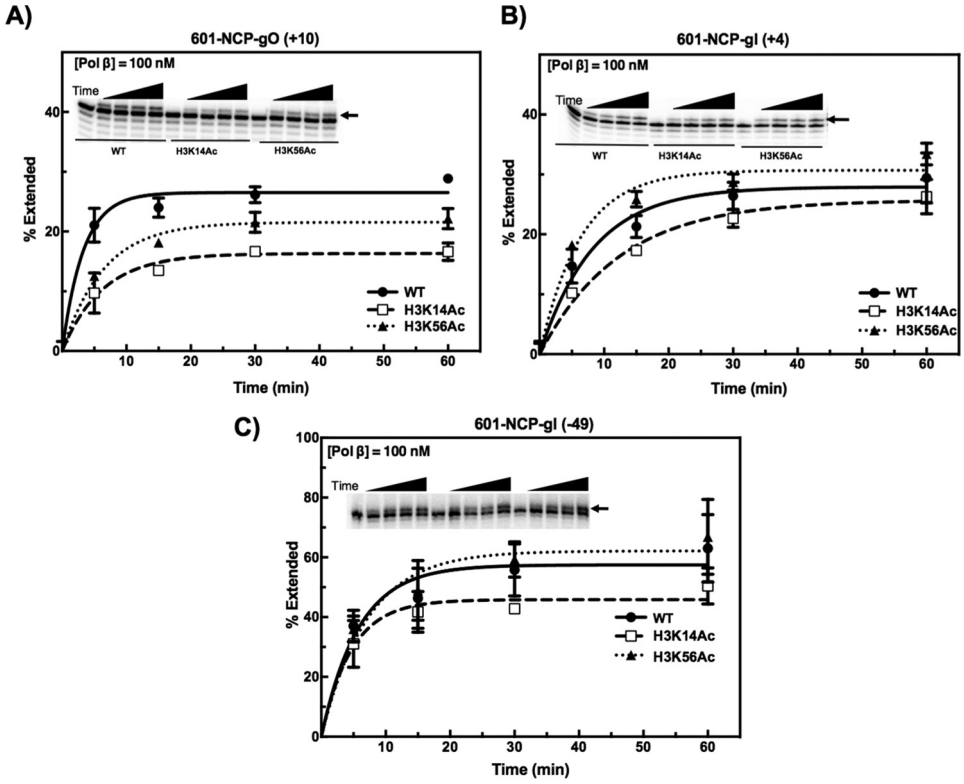

FIGURE 3. **Effect of histone site-specific acetylation on polymerase β gap-filling activity near the dyad and the DNA ends of nucleosomes.** Acetylated and unmodified NCPs containing a positioned single-nucleotide gap were incubated with Pol β at the specified concentrations. These concentrations of Pol β were at a 5-fold molar excess relative to nucleosomal DNA. Extension products were separated in 8% acrylamide denaturing sequencing gels. Representative gels (imbedded within each chart) are shown with an *arrow* denoting the extension product band. Data points represent the mean ± 1 S.D. of at least three independent experiments.

TABLE 1

Single-turnover kinetic summary for polymerase β extension in WT and site-specific acetylated nucleosome core particles

The initial rate of Pol β extension was calculated from the kinetic parameters obtained by fitting the data points in Fig. 3, *A–C*, to a single-phase exponential equation (solid/dashed curves). Initial rates were calculated from the product of the rate constants, k_{obs}, and their corresponding Y_{max} values. Errors represent the S.D. of each calculated rate.

Substrate	k_{obs}	Y_{max}	Initial rate
			% Extended/min
WT-NCP-gO (+10)	0.30 ± 0.05	26.5 ± 0.7	8.1 ± 1.3
H3K14Ac-gO (+10)	0.16 ± 0.03	16.3 ± 0.7	2.6 ± 0.5
H3K56Ac-gO (+10)	0.16 ± 0.02	21.6 ± 0.5	3.4 ± 0.3
WT-NCP-gI (+4)	0.12 ± 0.02	27.9 ± 1.3	3.4 ± 0.6
H3K14Ac-gI (+4)	0.08 ± 0.01	25.7 ± 1.0	2.1 ± 0.3
H3K56Ac-gI (+4)	0.16 ± 0.02	30.7 ± 0.9	4.9 ± 0.6
WT-NCP-gI (−49)	0.14 ± 0.03	62.8 ± 3.5	8.8 ± 2.0
H3K56Ac-NCP-gI (−49)	0.12 ± 0.02	68.8 ± 3.4	8.0 ± 1.5

To further examine the effect of H3K56Ac on structural dynamics, we measured the accessibility of two restriction enzymes (REs) to their target sites positioned near the ends of the DNA within NCPs. We found that the nucleosome dynamics within one turn of the DNA ends are increased at the *MSPI* target site due to H3K56Ac (Fig. 6*A*). However, accessibility to the HaeIII target site, which is only 9 bp upstream of the *MSPI* site, is unchanged (Fig. 6*B*). Because these lesions are located outside the range of increased dynamics observed in H3K56Ac-NCPs at position +61 (*MSP1* cut site), local structural changes beyond that of nucleosome breathing may accommodate Pol β binding and enzymatic activity. Together, these results indicate that acetylation may actually cause a reduction in lesion recognition and/or turnover of Pol β *in vitro* at a location near the dyad, NCP-gO (+10). This suggests that the Pol β "reading landscape" may be sensitive to local changes in electrostatic potential.

Previously we showed that nucleosome dynamics and stability are not changed by the presence of a single-nucleotide gap in the DNA (31). Given that H3K14Ac more significantly hinders accessibility to the single-nucleotide gap near the dyad (NCP-gO (+10)), we also measured RE accessibility in NCPs containing either WT or H3K14Ac octamers and a single nucleotide gap. NCPs were incubated with HaeIII, which cleaves near the end of the DNA (+51), or HhaI, which cleaves close to the dyad (+2). DNA cleavage by each of these REs is strongly inhibited by NCP formation (31, 47). Thus, we used this RE assay to determine if differences in NCP dynamics exist between WT and H3K14-acetylated NCPs that may explain the variation in Pol β extension activity. Not unexpectedly, we found that RE site accessibility is not significantly changed in H3K14Ac NCPs containing a single nucleotide gap (supplemental Figs. S5 and S6). These results suggest that histone acetylation may regulate Pol β recruitment or activity, independent of DNA accessibility.

Discussion

Posttranslational modifications of histones are crucial regulators of many DNA-templated processes, as they play a key role in regulating changes in the structure and dynamics of chromatin necessary for enzyme accessibility to DNA. Previous studies

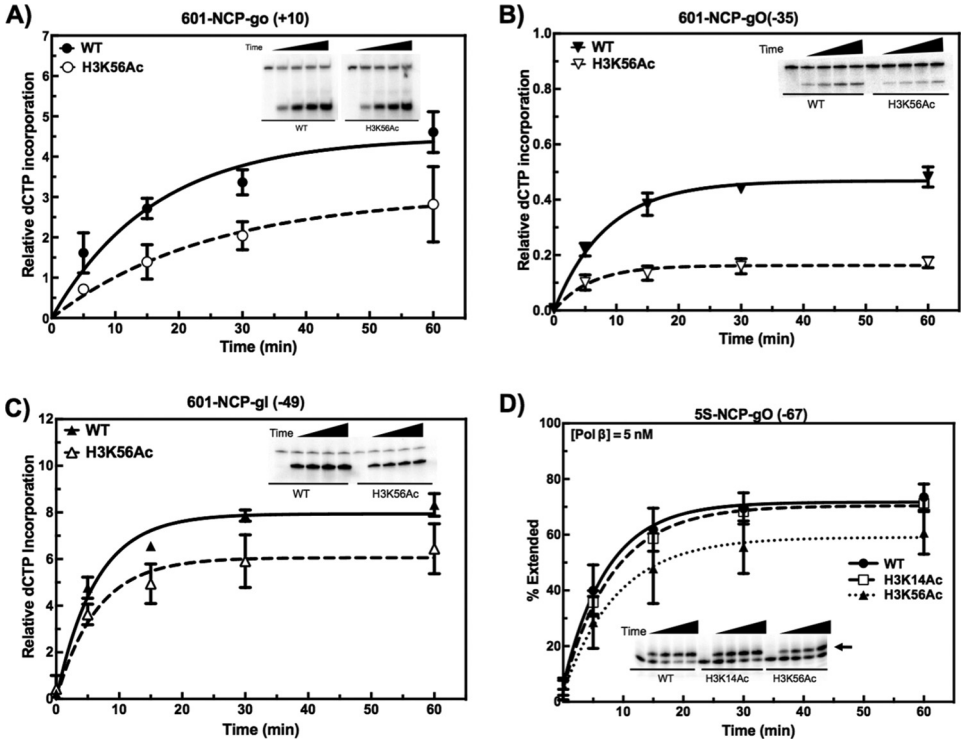

FIGURE 4. **Effect of H3K56 acetylation on polymerase β gap-filling activity near the nucleosome DNA ends.** *A–C*, the undamaged DNA strand, complementary to the strand containing a single-nucleotide gap, was labeled at its 5′ end with [γ-^{32}P]ATP. The DNA was then pretreated with UDG (30 nM) and APE1 (10 nM) to generate the single-nucleotide gap. The gap-containing DNA was reconstituted with WT (unmodified) or H3K14Ac histone octamers, and the resulting NCPs were incubated with 5 nM Pol β (where NCPs are at a 4-fold molar excess relative to Pol β) for the specified times at 37 °C. Gap-filling by Pol β was assessed by incorporation of [α^{32}P]dCTP (faster migrating band). *D*, a one-label assay was used where the gap-containing DNA strand was labeled at its 5′ end with [γ-^{32}P]ATP, and DNA synthesis was assessed by the appearance of a slower migrating band as indicated by the *arrow* relative to the total substrate. Data points represent the mean ± 1 S.D. of at least three independent experiments, and the *solid curves* are the kinetic fits of the data to a single-phase exponential equation, $Y = Y_{max}(1 - e^{-k_{obs}t})$. The initial rates were determined by solving the first derivative of the equation for time = 0, with initial rates in of 0.28 ± 0.08 and 0.12 ± 0.02 relative dCTP incorporation (RdI)/min^{-1} for WT-NCP-gO (+10) and H3K56Ac-NCP-gO (+10), respectively (*A*), 0.06 ± 0.005 RdI/min for WT-NCP-gO (−35) and 0.03 ± 0.006 RdI/min for H3K56Ac-NCP-gO (*B*), and 1.27 ± 0.14 for WT-NCP-gI (−49) and 0.94 ± 0.23 for H3K56Ac-NCP-gI (−49) (*C*). In *D* initial rates were independent of histone acetylation status, ~ 8.3 ± 1.4% extended/min. For data points where no error bars were visible, the S.D. was smaller or similar in magnitude to the size of the symbol.

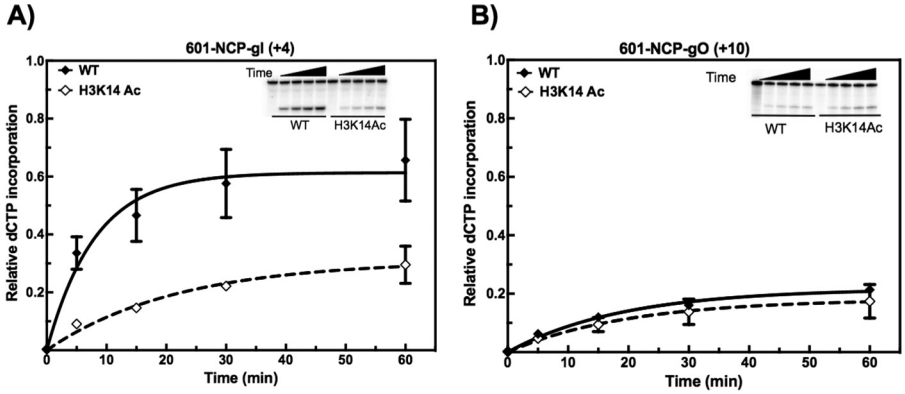

FIGURE 5. **Effect of H3K14 acetylation on polymerase β gap-filling activity near the nucleosome dyad using a two-label assay.** The undamaged DNA strand, complementary to the strand containing a single-nucleotide gap, was labeled at its 5′ end with [γ-^{32}P]ATP. The DNA was then pretreated with UDG (30 nM) and APE1 (10 nM) to generate the single-nucleotide gap. The gap-containing DNA was reconstituted with WT (unmodified) or H3K14Ac histone octamers, and the resulting NCPs were incubated with 5 nM Pol β (where NCPs are at a 4-fold molar excess relative to Pol β) for the specified times at 37 °C. Gap-filling by Pol β was assessed by incorporation of [α^{32}P]dCTP (faster migrating band). This signal intensity was then normalized to the signal intensity of the undamaged strand (slower migrating band). Data points represent the mean ± 1 S.D. of at least three independent experiments, and the *solid curves* are kinetic fits of the data to a single-phase exponential equation, $Y = Y_{max}(1 - e^{-k_{obs}t})$. *A*, the initial rate was determined by solving the first derivative of the equation for time = 0, with initial rates in of 0.08 ± 0.02 and 0.01 ± 0.003 relative dCTP incorporation/min^{-1} for WT-NCP-gI (+4) and H3K14Ac-NCP-gI (+4), respectively. There was no difference in the initial rate of WT and H3K14Ac at NCP-gO in *B*, with both having an initial rate of ~0.01 ± 0.002 relative dCTP incorporation/min. For data points where no error bars were visible, the S.D. was smaller or similar in magnitude to the size of the symbol.

have found that histone site-specific acetylation is important for the efficient repair of DSBs and UV-induced lesions (11). Importantly, there is some evidence that histone site-specific acetylation may be involved in BER (40, 41). However, a definitive role has not been established given that these PTMs are dynamic and exert combinatorial effects. Additionally, conflict-

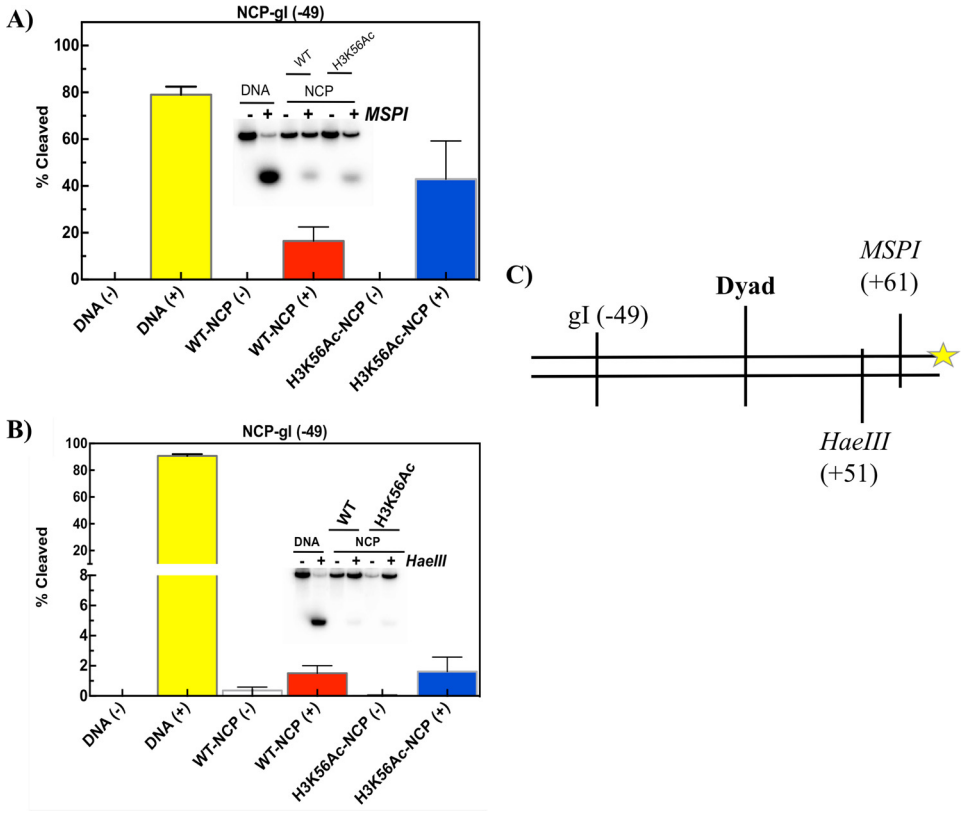

FIGURE 6. **Restriction enzyme accessibility assay on intact and gapped nucleosomal DNA containing WT (unmodified) or H3K14ac histone octamers.** Samples were incubated with restriction enzymes where indicated (+) at 37 °C for 2 h with either *MSPI* (*A*) or HaeIII (*B*). *Panel C* shows the cleavage sites of these REs relative to the DNA gap at −49. Representative 16% polyacrylamide gels are embedded within each chart. The histogram represents the mean of at least three independent experiments +1 S.D.

ing findings on the role of histone site-specific acetylation further illustrates the complexity of these studies in whole cells. For example, a large scale antibody-based screen for DNA damage-responsive histone modification in human cells found that acetylation levels at lysine 9 and 56 of histone H3 decrease in response to a wide range of DNA-damaging agents, including UV, MMS, and H_2O_2 (55). However, in another study, H3K56Ac levels increased in response to DNA damage in a dose-dependent manner (11). Because histone PTMs are more likely to be influenced by the histone-modification microenvironment, attributing a global response to a specific site of modification is quite challenging. Therefore, *in vitro* studies are advantageous in the sense that they eliminate many unknowns. Thus, in this study we focused on two structurally distinct sites of histone acetylation that have been implicated in DNA repair processes: H3K14 and H3K56.

We found that histone H3 Lys-14 and Lys-56 acetylation do not affect the initial cleavage steps of BER in nucleosomes. This is the case for DNA sequences with a range of differing NCP-positioning strengths (601, 5S rDNA, and TG motif) (56). These results suggest that acetylation alone at H3K14 or H3K56 does not induce the local structural and/or dynamic changes necessary to increase the accessibility to uracil by UDG. This is in agreement with the ·OH radical footprinting data (supplemental Fig. S2) and RE accessibility assays (supplemental Figs. S5 and S6) of WT and H3K14Ac NCPs showing no significant difference in cleavage pattern and target site cleavage, respectively. Given that H3K14Ac is located in the H3 N-terminal tail, it is not surprising that this modification alone does not induce detectible histone-DNA disruptions.

Surprisingly, we found that acetylation of H3 Lys-14 or Lys-56 decreases gap-filling DNA synthesis by Pol β. Because these histone acetylation sites are primarily associated with different repair pathways (H3K14) or newly replicated DNA (H3K56), we propose that acetylation at these histone sites may inhibit Pol β activity to promote alternative gap-filling pathways (*e.g.* by a higher fidelity DNA polymerase). H3 K56Q mutants, which mimic constitutive Lys-56 acetylation, are hypersensitive to MMS in both yeast and mammalian cells (13, 52). Our data suggest that this MMS sensitivity may be in part due to inhibition of polymerase gap filling during BER. The H3 K56R mutant, which completely eliminates H3 Lys-56 acetylation, is also MMS-sensitive. However, this phenotype is likely due to the established role of H3 Lys-56 acetylation in replication-coupled nucleosome assembly (57) perhaps associated with recombination or long-patch BER repair DNA synthesis.

Our data indicate that deacetylation at H3K56 may be necessary to promote BER. SIRT6, an NAD^+-dependent histone/protein deacetylase and mono-ADP-ribosyltransferase, targets H3K56 for deacetylation, and ADP-ribosylates PARP1 to promote recruitment of downstream BER factors (58). SIRT6 deficiency leads to a phenotype that is consistent with BER defects (sensitivity to MMS, H_2O_2, and ionizing radiation) (40). Importantly, this sensitivity is rescued by overexpression of the active 8-kDa 5′-deoxyribose phosphate lyase domain of Pol β. Therefore, in the absence of SIRT6, where H3K56Ac persists, DNA

gaps may be shunted to another DNA polymerase that lacks 5′-deoxyribose phosphate lyase activity (*e.g.* Pol ϵ, which has been implicated in BER and S-phase checkpoint) (59). Alternatively, H3K56Ac may serve as a mark that recruits SIRT6 to sites of DNA damage, allowing it to directly modify BER factors via its dual enzymatic activities. In this scenario it activates PARP1 via its ADP-ribosyltransferase activity (39) and deacetylates H3K56Ac to allow this site to become ribosylated by PARP1 or SIRT6. Indeed, this may promote chromatin relaxation more efficiently than acetylation. In addition, because SIRT6 shows some *in vitro* deacetylase activity toward Pol β (40), which may increase in the context of NCPs, SIRT6-mediated deacetylation of Pol β may be important in regulating its activity.

Acetylation of either H3K14 or H3K56 decreases the gap-filling activity of Pol β at NCP-gO (+10) under conditions where Pol β is in excess relative to the NCP substrate (Fig. 3*A*). At this same location, when Pol β is limiting, only H3K56Ac decreased the Pol β activity (Fig. 4*A*). We also observed that H3K14Ac had no effect under steady-state conditions (Fig. 5*B*). The opposite was observed at NCP-gI (+4), where gap-filling activity was decreased only in conditions where Pol β is limiting and not when Pol β is in excess (Figs. 3*B* and 5*A*). These findings highlight the complex nature of Pol β activity on nucleosomes. Indeed, they reinforce our previous findings that the different structural locations of lesions within NCPs are associated with different rate-limiting constraints on Pol β activity (31). More importantly, these constraints are differentially modulated by the PTM status of histone H3, and acetylation at a particular site does not have a general effect on Pol β activity at lesions in nucleosomes. Instead, these modifications directly influence the binding or damage recognition by Pol β. At NCP-gO (+10), accessibility to or bending of the template strand by Pol β during synthesis is likely to be an important barrier that must be overcome for catalysis to occur. One possibility is that acetylation at H3K14 transiently changes the histone H3 tail interactions in this region. Indeed, it was previously shown that hyperacetylated N-terminal histone tails maintain contact with DNA, albeit to a lesser extent than unmodified tails, and the DNA interaction is structurally different from that of unacetylated tails (51). Given the location of H3K14 in the H3 N-terminal tail, it is possible that acetylation at this site transiently changes the positioning of the tail and interferes not only with accessibility to the DNA gap but also to the templating strand, particularly at NCP-gO (+10).

Our results were unexpected, as histone acetylation has long been linked to increased chromatin accessibility for DNA-templated processes. However, recent findings suggest a unique, indirect role for histone acetylation at H3K56 where deacetylation at this site is required for efficient DSB repair given that expression of H3K56Q mutant impairs repair; in this mutant a chromatin-modifier factor is presumably no longer able to induce chromatin relaxation (59). However these two activities (deacetylation and chromatin remodeling) occur in parallel, and thus they are both required for efficient repair. Furthermore, activation of PARP1 by the ADP-ribosyltransferase activity of SIRT6 has been reported to stimulate DSB repair (39). Therefore, ADP-ribosylation on PARP1 itself or at H3K56, which requires deacetylation before PARP1 activity, may serve as an alternative pathway for intrinsically regulating chromatin structure. Given that PARP1 is one of the first responders in BER that protects single-strand breaks (in the presence of H3K56Ac), it may not be able to rapidly carry out ADP-ribosylation at this site to induce early, rapid chromatin changes that allow the recruitment of Pol β. Thus, in this scenario, acetylation at H3K56 in the absence of SIRT6 may inhibit the recruitment and/or activity of Pol β. Consequently, H3K56 may not be sufficient to regulate chromatin structure for efficient BER in chromatin, and its deacetylation may be required for binding of additional repair factors.

Finally, some past reports also found decreased activity of DNA-templated processes in acetylated chromatin. For example, despite the well known role of H3K14Ac in transcriptional activation, it was recently reported that a subset of inactive promoters is selectively enriched for H3K14Ac in the mouse genome (60). In addition, histone hyperacetylation after exposure to sodium butyrate, an inhibitor of histone deacetylases, constrains DNA DSB repair in human lymphocytes (61). Taken together, our results indicate that the effects of histone site-specific acetylation are more complex than the simple model where increased acetylation yields greater DNA accessibility and thus more efficient DNA repair. Considering the heavy presence of acetylated histones in some regions of the genome, there remains a compelling need for future investigations on the mechanism by which site-specific histone acetylation influences BER. Indeed, understanding the regulation of BER by histone PTMs could provide important insights into the mechanisms in the emerging field of HDAC inhibitors as promising cancer therapeutic agents.

Author Contributions—Y. R. coordinated the study, performed the experiments with 601- and 5S-NCPs, and co-wrote the paper. J. M. H. provided technical assistance, contributed to the experiments using the TG nucleosomes, and edited the paper. M. F. L. and J. J. W. performed all yeast experiments and co-wrote the paper, respectively. M. J. S. conceived the study, provided feedback during the study, and co-wrote the paper. All authors reviewed the results and approved the final version of the manuscript.

Acknowledgments—We thank Drs. Samuel H. Wilson and Rajendra Prasad (Laboratory of Structural Biology, NIEHS) for providing human DNA Polymerase β. We thank Amelia Hodges for technical assistance.

References

1. Luger, K., Mäder, A. W., Richmond, R. K., Sargent, D. F., and Richmond, T. J. (1997) Crystal structure of the nucleosome core particle at 2.8 Å resolution. *Nature* **389,** 251–260
2. Varga-Weisz, P. (2001) ATP-dependent chromatin remodeling factors: nucleosome shufflers with many missions. *Oncogene* **20,** 3076–3085
3. Swygert, S. G., and Peterson, C. L. (2014) Chromatin dynamics: interplay between remodeling enzymes and histone modifications. *Biochim. Biophys. Acta* **1839,** 728–736
4. North, J. A., Shimko, J. C., Javaid, S., Mooney, A. M., Shoffner, M. A., Rose, S. D., Bundschuh, R., Fishel, R., Ottesen, J. J., and Poirier, M. G. (2012) Regulation of the nucleosome unwrapping rate controls DNA accessibility. *Nucleic Acids Res.* **40,** 10215–10227
5. Li, G., Levitus, M., Bustamante, C., and Widom, J. (2005) Rapid spontane-

ous accessibility of nucleosomal DNA. *Nat. Struct. Mol. Biol.* **12,** 46–53
6. Anderson, J. D., and Widom, J. (2000) Sequence and position-dependence of the equilibrium accessibility of nucleosomal DNA target sites. *J. Mol. Biol.* **296,** 979–987
7. Polach, K. J., and Widom, J. (1995) Mechanism of protein access to specific DNA sequences in chromatin: a dynamic equilibrium model for gene regulation. *J. Mol. Biol.* **254,** 130–149
8. Tims, H. S., and Widom, J. (2007) Stopped-flow fluorescence resonance energy transfer for analysis of nucleosome dynamics. *Methods* **41,** 296–303
9. Neumann, H., Hancock, S. M., Buning, R., Routh, A., Chapman, L., Somers, J., Owen-Hughes, T., van Noort, J., Rhodes, D., and Chin, J. W. (2009) A method for genetically installing site-specific acetylation in recombinant histones defines the effects of H3 Lys-56 acetylation. *Mol. Cell* **36,** 153–163
10. Shimko, J. C., North, J. A., Bruns, A. N., Poirier, M. G., and Ottesen, J. J. (2011) Preparation of fully synthetic histone H3 reveals that acetyl-lysine 56 facilitates protein binding within nucleosomes. *J. Mol. Biol.* **408,** 187–204
11. Das, C., Lucia, M. S., Hansen, K. C., and Tyler, J. K. (2009) CBP/p300-mediated acetylation of histone H3 on lysine 56. *Nature* **459,** 113–117
12. Schneider, J., Bajwa, P., Johnson, F. C., Bhaumik, S. R., and Shilatifard, A. (2006) Rtt109 is required for proper H3K56 acetylation: a chromatin mark associated with the elongating RNA polymerase II. *J. Biol. Chem.* **281,** 37270–37274
13. Masumoto, H., Hawke, D., Kobayashi, R., and Verreault, A. (2005) A role for cell-cycle-regulated histone H3 lysine 56 acetylation in the DNA damage response. *Nature* **436,** 294–298
14. Vempati, R. K., Jayani, R. S., Notani, D., Sengupta, A., Galande, S., and Haldar, D. (2010) p300-mediated acetylation of histone H3 lysine 56 functions in DNA damage response in mammals. *J. Biol. Chem.* **285,** 28553–28564
15. Miller, K. M., Maas, N. L., and Toczyski, D. P. (2006) Taking it off: regulation of H3 Lys-56 acetylation by Hst3 and Hst4. *Cell Cycle* **5,** 2561–2565
16. Maas, N. L., Miller, K. M., DeFazio, L. G., and Toczyski, D. P. (2006) Cell cycle and checkpoint regulation of histone H3 Lys-56 acetylation by Hst3 and Hst4. *Mol. Cell* **23,** 109–119
17. Ozdemir, A., Masumoto, H., Fitzjohn, P., Verreault, A., and Logie, C. (2006) Histone H3 lysine 56 acetylation: a new twist in the chromosome cycle. *Cell Cycle* **5,** 2602–2608
18. Wurtele, H., Kaiser, G. S., Bacal, J., St-Hilaire, E., Lee, E. H., Tsao, S., Dorn, J., Maddox, P., Lisby, M., Pasero, P., and Verreault, A. (2012) Histone H3 lysine 56 acetylation and the response to DNA replication fork damage. *Mol. Cell. Biol.* **32,** 154–172
19. Simon, M., North, J. A., Shimko, J. C., Forties, R. A., Ferdinand, M. B., Manohar, M., Zhang, M., Fishel, R., Ottesen, J. J., and Poirier, M. G. (2011) Histone fold modifications control nucleosome unwrapping and disassembly. *Proc. Natl. Acad. Sci. U.S.A.* **108,** 12711–12716
20. Kasten, M., Szerlong, H., Erdjument-Bromage, H., Tempst, P., Werner, M., and Cairns, B. R. (2004) Tandem bromodomains in the chromatin remodeler RSC recognize acetylated histone H3 Lys14. *EMBO J.* **23,** 1348–1359
21. VanDemark, A. P., Kasten, M. M., Ferris, E., Heroux, A., Hill, C. P., and Cairns, B. R. (2007) Autoregulation of the rsc4 tandem bromodomain by gcn5 acetylation. *Mol. Cell* **27,** 817–828
22. Wang, Y., Kallgren, S. P., Reddy, B. D., Kuntz, K., López-Maury, L., Thompson, J., Watt, S., Ma, C., Hou, H., Shi, Y., Yates, J. R., 3rd, Bähler, J., O'Connell, M. J., and Jia, S. (2012) Histone H3 lysine 14 acetylation is required for activation of a DNA damage checkpoint in fission yeast. *J. Biol. Chem.* **287,** 4386–4393
23. Yu, Y., Teng, Y., Liu, H., Reed, S. H., and Waters, R. (2005) UV irradiation stimulates histone acetylation and chromatin remodeling at a repressed yeast locus. *Proc. Natl. Acad. Sci. U.S.A.* **102,** 8650–8655
24. Luebben, W. R., Sharma, N., and Nyborg, J. K. (2010) Nucleosome eviction and activated transcription require p300 acetylation of histone H3 lysine 14. *Proc. Natl. Acad. Sci. U.S.A.* **107,** 19254–19259
25. van Attikum, H., and Gasser, S. M. (2009) Crosstalk between histone modifications during the DNA damage response. *Trends Cell Biol.* **19,** 207–217
26. Baute, J., and Depicker, A. (2008) Base excision repair and its role in maintaining genome stability. *Crit. Rev. Biochem. Mol. Biol.* **43,** 239–276
27. Hegde, M. L., Hazra, T. K., and Mitra, S. (2008) Early steps in the DNA base excision/single-strand interruption repair pathway in mammalian cells. *Cell Res.* **18,** 27–47
28. Zharkov, D. O. (2008) Base excision DNA repair. *Cell. Mol. Life Sci.* **65,** 1544–1565
29. Fromme, J. C., and Verdine, G. L. (2004) Base excision repair. *Adv. Protein Chem.* **69,** 1–41
30. Robertson, A. B., Klungland, A., Rognes, T., and Leiros, I. (2009) DNA repair in mammalian cells: base excision repair: the long and short of it. *Cell. Mol. Life Sci.* **66,** 981–993
31. Rodriguez, Y., and Smerdon, M. J. (2013) The structural location of DNA lesions in nucleosome core particles determines accessibility by base excision repair enzymes. *J. Biol. Chem.* **288,** 13863–13875
32. Beard, B. C., Wilson, S. H., and Smerdon, M. J. (2003) Suppressed catalytic activity of base excision repair enzymes on rotationally positioned uracil in nucleosomes. *Proc. Natl. Acad. Sci. U.S.A.* **100,** 7465–7470
33. Cole, H. A., Tabor-Godwin, J. M., and Hayes, J. J. (2010) Uracil DNA glycosylase activity on nucleosomal DNA depends on rotational orientation of targets. *J. Biol. Chem.* **285,** 2876–2885
34. Odell, I. D., Barbour, J. E., Murphy, D. L., Della-Maria, J. A., Sweasy, J. B., Tomkinson, A. E., Wallace, S. S., and Pederson, D. S. (2011) Nucleosome disruption by DNA ligase III-XRCC1 promotes efficient base excision repair. *Mol. Cell. Biol.* **31,** 4623–4632
35. Menoni, H., Gasparutto, D., Hamiche, A., Cadet, J., Dimitrov, S., Bouvet, P., and Angelov, D. (2007) ATP-dependent chromatin remodeling is required for base excision repair in conventional but not in variant H2A.Bbd nucleosomes. *Mol. Cell. Biol.* **27,** 5949–5956
36. Hinz, J. M., Rodriguez, Y., and Smerdon, M. J. (2010) Rotational dynamics of DNA on the nucleosome surface markedly impact accessibility to a DNA repair enzyme. *Proc. Natl. Acad. Sci. U.S.A.* **107,** 4646–4651
37. Prasad, A., Wallace, S. S., and Pederson, D. S. (2007) Initiation of base excision repair of oxidative lesions in nucleosomes by the human, bifunctional DNA glycosylase NTH1. *Mol. Cell. Biol.* **27,** 8442–8453
38. Hinz, J. M. (2014) Impact of abasic site orientation within nucleosomes on human APE1 endonuclease activity. *Mutat. Res.* **766,** 19–24
39. Mao, Z., Hine, C., Tian, X., Van Meter, M., Au, M., Vaidya, A., Seluanov, A., and Gorbunova, V. (2011) SIRT6 promotes DNA repair under stress by activating PARP1. *Science* **332,** 1443–1446
40. Mostoslavsky, R., Chua, K. F., Lombard, D. B., Pang, W. W., Fischer, M. R., Gellon, L., Liu, P., Mostoslavsky, G., Franco, S., Murphy, M. M., Mills, K. D., Patel, P., Hsu, J. T., Hong, A. L., Ford, E., *et al.* (2006) Genomic instability and aging-like phenotype in the absence of mammalian SIRT6. *Cell* **124,** 315–329
41. Hwang, B. J., Jin, J., Gao, Y., Shi, G., Madabushi, A., Yan, A., Guan, X., Zalzman, M., Nakajima, S., Lan, L., and Lu, A. L. (2015) SIRT6 protein deacetylase interacts with MYH DNA glycosylase, APE1 endonuclease, and Rad9-Rad1-Hus1 checkpoint clamp. *BMC Mol. Biol.* **16,** 12
42. Lowary, P. T., and Widom, J. (1998) New DNA sequence rules for high affinity binding to histone octamer and sequence-directed nucleosome positioning. *J. Mol. Biol.* **276,** 19–42
43. Fernandez, A. G., and Anderson, J. N. (2007) Nucleosome positioning determinants. *J. Mol. Biol.* **371,** 649–668
44. Vasudevan, D., Chua, E. Y., and Davey, C. A. (2010) Crystal structures of nucleosome core particles containing the '601' strong positioning sequence. *J. Mol. Biol.* **403,** 1–10
45. Mann, D. B., Springer, D. L., and Smerdon, M. J. (1997) DNA damage can alter the stability of nucleosomes: effects are dependent on damage type. *Proc. Natl. Acad. Sci. U.S.A.* **94,** 2215–2220
46. Luger, K., Rechsteiner, T. J., and Richmond, T. J. (1999) Preparation of nucleosome core particle from recombinant histones. *Methods Enzymol.* **304,** 3–19
47. Duan, M. R., and Smerdon, M. J. (2010) UV damage in DNA promotes nucleosome unwrapping. *J. Biol. Chem.* **285,** 26295–26303
48. Tullius, T. D. (1991) DNA footprinting with the hydroxyl radical. *Free*

Radic. Res. Commun. **12,** 521–529
49. Donigan, K. A., Sun, K. W., Nemec, A. A., Murphy, D. L., Cong, X., Northrup, V., Zelterman, D., and Sweasy, J. B. (2012) Human POLB gene is mutated in high percentage of colorectal tumors. *J. Biol. Chem.* **287,** 23830–23839
50. Hodges, A. J., Gallegos, I. J., Laughery, M. F., Meas, R., Tran, L., and Wyrick, J. J. (2015) Histone sprocket arginine residues are important for gene expression, DNA repair, and cell viability in *Saccharomyces cerevisiae*. *Genetics* **200,** 795–806
51. Mutskov, V., Gerber, D., Angelov, D., Ausio, J., Workman, J., and Dimitrov, S. (1998) Persistent interactions of core histone tails with nucleosomal DNA following acetylation and transcription factor binding. *Mol. Cell. Biol.* **18,** 6293–6304
52. Yuan, J., Pu, M., Zhang, Z., and Lou, Z. (2009) Histone H3-K56 acetylation is important for genomic stability in mammals. *Cell Cycle* **8,** 1747–1753
53. Driscoll, R., Hudson, A., and Jackson, S. P. (2007) Yeast Rtt109 promotes genome stability by acetylating histone H3 on lysine 56. *Science* **315,** 649–652
54. Liu, X., and Smerdon, M. J. (2000) Nucleotide excision repair of the 5 S ribosomal RNA gene assembled into a nucleosome. *J. Biol. Chem.* **275,** 23729–23735
55. Tjeertes, J. V., Miller, K. M., and Jackson, S. P. (2009) Screen for DNA-damage-responsive histone modifications identifies H3K9Ac and H3K56Ac in human cells. *EMBO J.* **28,** 1878–1889
56. Widlund, H. R., Cao, H., Simonsson, S., Magnusson, E., Simonsson, T., Nielsen, P. E., Kahn, J. D., Crothers, D. M., and Kubista, M. (1997) Identification and characterization of genomic nucleosome-positioning sequences. *J. Mol. Biol.* **267,** 807–817
57. Li, Q., Zhou, H., Wurtele, H., Davies, B., Horazdovsky, B., Verreault, A., and Zhang, Z. (2008) Acetylation of histone H3 lysine 56 regulates replication-coupled nucleosome assembly. *Cell* **134,** 244–255
58. Xu, Z., Zhang, L., Zhang, W., Meng, D., Zhang, H., Jiang, Y., Xu, X., Van Meter, M., Seluanov, A., Gorbunova, V., and Mao, Z. (2015) SIRT6 rescues the age related decline in base excision repair in a PARP1-dependent manner. *Cell Cycle* **14,** 269–276
59. Garcia-Diaz, M., and Bebenek, K. (2007) Multiple functions of DNA polymerases. *CRC Crit. Rev. Plant Sci.* **26,** 105–122
60. Karmodiya, K., Krebs, A. R., Oulad-Abdelghani, M., Kimura, H., and Tora, L. (2012) H3K9 and H3K14 acetylation co-occur at many gene regulatory elements, while H3K14ac marks a subset of inactive inducible promoters in mouse embryonic stem cells. *BMC Genomics* **13,** 424
61. Stoilov, L., Darroudi, F., Meschini, R., van der Schans, G., Mullenders, L. H., and Natarajan, A. T. (2000) Inhibition of repair of X-ray-induced DNA double-strand breaks in human lymphocytes exposed to sodium butyrate. *Int. J. Radiat. Biol.* **76,** 1485–1491